Nanoscale

PAPER

View Article Online
View Journal | View Issue

Cite this: *Nanoscale*, 2019, **11**, 1074

Characterizing percolative materials by straining†

Heming Yao, [a] Marek Hempel, [b] Ya-Ping Hsieh,[c] Jing Kong[b] and Mario Hofmann *[d]

Received 12th November 2018,
Accepted 6th December 2018

DOI: 10.1039/c8nr09120j

rsc.li/nanoscale

Carrier transport in a wide range of nanomaterial assemblies proceeds by percolation through discontinuous networks of constituents. Improving percolative nanomaterials could enhance transparent conductors, sensors, and electronic devices. A significant obstacle in optimizing percolative materials is the challenge in their characterization. The critical connection pathways which determine a percolative material's conductivity are not easily accessible with existing metrology tools and traditional investigation approaches rely on indirect methods based on many samples and on simplifying assumptions. We here demonstrate the direct extraction of characteristic parameters from a single sample by analyzing the strain-dependent resistance of percolative materials. An analytical model is derived that can explain experimental data for various percolative materials, morphologies, and straining conditions. The relationship of the extracted parameters with previously introduced figures of merit allows us to compare nanostructures of diverse dimensionalities and compositions for applications such as strain gauges and transparent conductors.

Introduction

Assemblies of nanomaterials have demonstrated novel and unique properties in energy storage,[1] sensing,[2] and biological,[3] and electronic devices.[4] One important distinction from their bulk counterpart is that carrier transport proceeds through discrete constituents. This percolative transport is determined by the geometry of their constituents and the morphology of their assembly. Despite the significant effort invested into the fabrication and application of percolative films, fundamental questions about the best material, ideal geometry and performance limits have remained unanswered. Such questions could be answered with either theoretical or experimental approaches. Simulations on percolative transport to date have only been conducted on simple geometries, such as nanowires[5] or circles,[6] and cannot explain the richness of experimental observations, such as non-universal percolation exponents and large variations between seemingly identical samples.[7] Experimental characterization of percolative films by imaging[8] or scanning probe microscopy[9] on the other hand is complicated since such an analysis has to consider both the properties of individual constituents and the macroscopic conduction pathways. This disparity between scales is causing severe challenges to the metrology and characterization of percolative films.

Traditionally, the percolative transport is described by two parameters, *i.e.* the percolation exponent and a critical film thickness under which no conduction occurs. The comparison of these parameters can allow the harmonization between different materials and the evaluation of optimal morphologies. Unfortunately, the parameters are not directly measurable and need to be extracted from multiple samples which is both time-consuming and produces large errors in the analysis. Moreover, the method produces larger errors the closer the film thickness is to the critical thickness which limits its suitability for envisioned nanomaterials' applications, such as strain sensors,[10] electronic skin[11] or transparent ESD protection.[12]

Previous work has demonstrated the sensitivity of a percolative film's morphology to uniaxial strain which was ascribed to the reorientation of its constituents upon extension and related to the film's percolation parameters.[13,14]

We here extract the percolation parameters of nanostructure films from strain-dependent conductance measurements. For this, we analyze the carrier transport of percolative films under tensile strain and present a simple analytical formula that predicts the percolation process at varying degrees of strain. This result enables the extraction of the fundamental parameters of these films, such as the percolation exponent and the critical thickness from one sample without additional characterization

[a]*Department of Electrical and Electronic Engineering, The University of Hong Kong, Hong Kong. E-mail: Mario@phys.ntu.edu.tw*
[b]*Department of Electrical Engineering and Computer Science, Massachusetts Institute of Technology, Cambridge, USA*
[c]*Institute for Atomic and Molecular Sciences, Academia Sinica, Taipei, Taiwan*
[d]*Department of Physics, National Taiwan University, Taipei, Taiwan*
†Electronic supplementary information (ESI) available. See DOI: 10.1039/c8nr09120j

tools. The presented model is shown to be applicable to a wide variety of nanomaterials, such as graphene flakes, nanotubes and nanoparticles. Moreover, the previously proposed figure of merit for percolative films can be obtained in a straightforward manner without additional assumptions. Finally, the application of our model to recently developed strain sensors can provide a pathway for their optimization.

Results and discussion

The traditional characterization of percolative films is based on the comparison of multiple samples with varying concentrations of nanostructures. Fig. 1(a) shows the resistance evolution of samples with progressively increasing amounts of graphene flakes deposited. This change can be understood by the increase in flake concentration that yields a larger number of parallel conduction pathways. To relate the sample resistance to the film morphology, optical absorption measurements need to be carried out for each sample and an increase in absorbance with the deposited volume can be seen (Fig. 1(b)). These two measurements allow the inference of a trend between a sample's absorbance and resistance (Fig. 1(c)).[8,11,15–17] For nanomaterials, this relationship is not a simple inverse proportionality as expected for bulk materials,[8] which is indicated by the observation that films that exhibit less than 50% absorbance do not conduct current because the film fails to form an interconnected network.[8,11] Employing this critical thickness, a power-law dependence of resistance is commonly employed to describe percolation[8,11,16–18]:

$$\rho_{DC} \propto \left(\frac{t}{t_c} - 1\right)^{-n} \quad (1)$$

Here n is the percolation exponent which represents the abruptness of the transition between hopping and bulk conduction and is affected by the geometry, conduction mechanism, and dimensionality of the film components.[7,19–25] Early theoretical work found universal percolation exponents that depended predominantly on the dimensionality of the problem with n = 1.1–1.3 for two-dimensional systems and n = 1.6–2.0 for three-dimensional systems. Experimental work demonstrated exponents within a much larger range between 2 and 10 that depended on the aspect ratio of the constituents and the hopping resistance between neighboring elements.[7] Even for seemingly similar carbon nanotube films large spreads of values have been reported,[7] indicating the importance of extracting an accurate value for the percolation exponent.

Fits of the experimental data with eqn (1) demonstrate large deviations between the data and model resulting in unreasonable thickness values below the critical thickness (Fig. 1(d)). The deviation of experimental values originates from the assumption that the critical thickness and percolation exponent n are similar for all samples. Instead, irreproducible deposition and changes in the sample morphology cannot be ignored in nanostructure assemblies.[7,8,15,22,26] Thus, a method is needed that can extract the same information from the measurement of a single sample and would not need to rely on assumptions

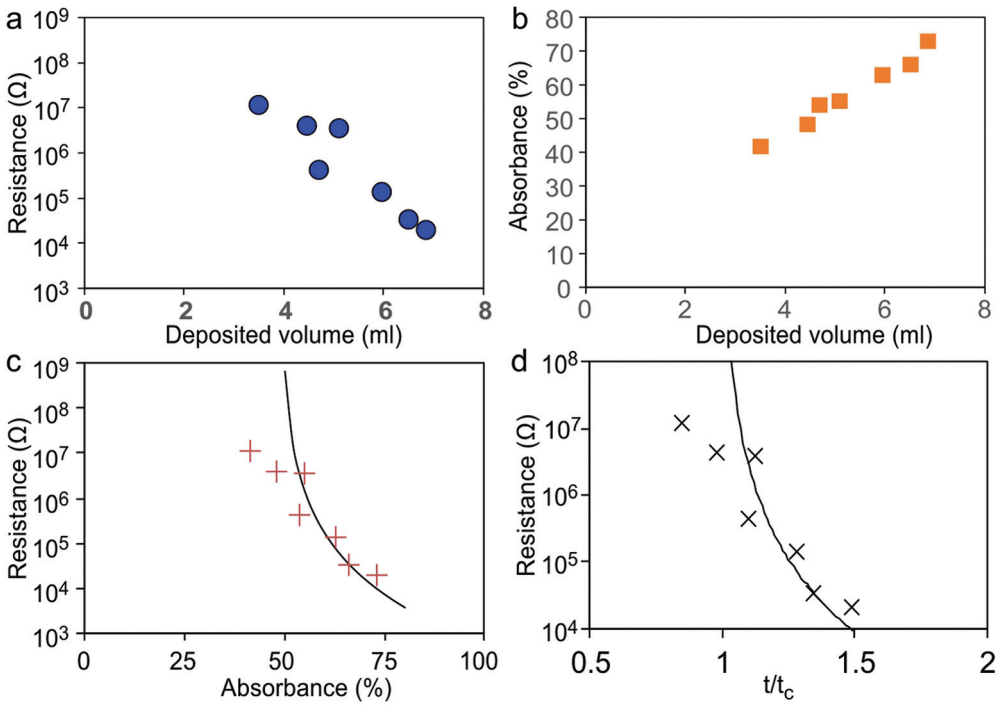

Fig. 1 (a) Resistance of graphene flake films deposited from different volumes of solution, (b) dependence of optical absorbance at 532 nm on the amount of deposited volume, (c) resistance *vs.* optical absorbance for samples with different thicknesses with fitting to the percolation equation, and (d) resistance *vs.* extracted normalized thickness with fitting to the percolation equation.

about the sample variation. Moreover, a single-sample measurement could be conducted without the knowledge of the sample thickness since it could be treated as a constant.

We hypothesize that straining a sample could modify its response in a predictable manner that allows the extraction of the percolation parameters. Application of uniaxial strain ε to a percolative sample is expected to change the position of the film's constituents while retaining its shape, due to the high strength of the conductive constituent compared to the dielectric matrix.[27] Under these conditions, strain will change the percolation conditions significantly since constituents will be shifted with respect to each other resulting in broken conduction pathways. To illustrate this process, we conduct numerical simulations of the current flow through a collection of conductive disks by solving Kirchhoff's law for each junction,[28] presented in Fig. 2(a). A uniaxial variation of the positions is found to decrease the density of conduction pathways, thus resulting in an increased total resistance.

We analytically model this behavior by considering the changes in the sample. Assuming elastic strain and the above-mentioned conservation of the conductive constituent volume under strain, the modification of the sample's cross-sectional area causes a decrease of the film thickness, according to

$$t(\varepsilon) = t_0/(1+\varepsilon)(1-\mu\varepsilon), \tag{2}$$

where ε is strain, μ is Poisson's ratio and t_0 is the original film thickness $t(\varepsilon = 0)$. (More details on the model are presented in the ESI.†)

We thus find that the application of strain to a sample has the same effect as changing its thickness. Consequently, the resistance of one sample under different degrees of strain can yield the same amount of information as that obtained by measuring the resistance of many samples with varying thickness. Since the critical thickness of the film does not depend on strain but only on dimensionality and conductivity,[19,29] this approach is expected to reduce the error in the extracted parameters compared to multi-sample measurements.

Experimentally measured sample resistances have to consider strain induced changes in length (L), width (W), conductivity (σ_{DC}) and film thickness according to

$$R = \left(\frac{L(\varepsilon)}{W(\varepsilon)}\right)(\sigma_{DC}(\varepsilon)t(\varepsilon))^{-1} \tag{3}$$

By normalizing the resistance of the unstrained sample, we obtain a simple analytical equation that allows us to extract important percolation parameters such as the percolation exponent (n) and the critical film thickness (t_c) with respect to the unstrained film thickness (t_0) from a single measurement.

$$R(\varepsilon)/R(0) = \left(\frac{t_0 - t_c}{t(\varepsilon) - t_c}\right)^n (1+\varepsilon)^2, \tag{4}$$

where $t(\varepsilon)$ is the strain-dependent thickness according to eqn (2).

The experimental confirmation of our newly proposed method is firstly carried out on percolative graphene flake

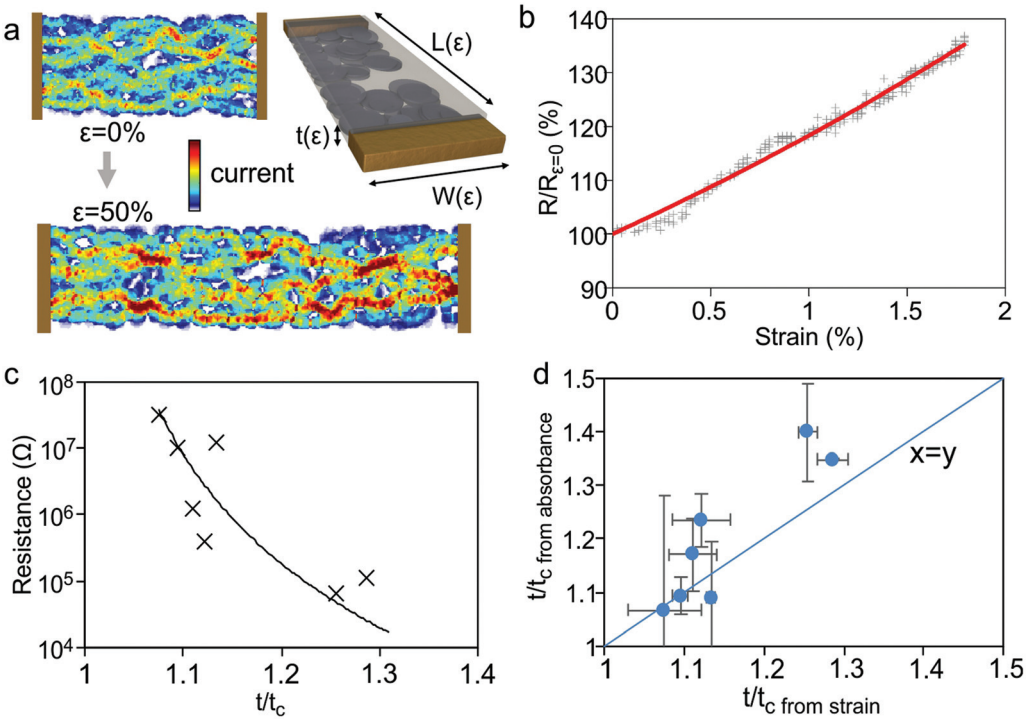

Fig. 2 (a) Schematic of the strain-induced changes in percolative films and numerical simulation of current distribution in the same percolative film with and without strain, (b) representative normalized strain–resistance curve for a graphene flake film with fitting to eqn (4) with parameters n = 2.4 and t/t_c = 1.25, (c) resistance *vs.* extracted normalized thickness from strain–resistance measurements with fitting to the percolation equation, and (d) relationship between the normalized thickness obtained from strain measurements and multi-sample optical transmittance measurements.

films. These films were obtained by spray deposition of exfoliated graphene from NMP on a flexible PET substrate.[28] We observe a good agreement between the experimental strain-resistance graph and eqn (4) (Fig. 2(b)). From the fit we can extract the percolation exponent n and the normalized thickness t/t_c, which are sufficient to describe the percolative behavior of a film.

To rationalize the extracted parameters, we compare graphene flake films of different thicknesses. When plotting the extracted normalized thickness t/t_c for each sample, a clear trend with its initial resistance is observed (Fig. 2(c)), consistent with the results obtained by absorption measurements of multiple samples in Fig. 1(d). We compare the extracted normalized thicknesses from traditional multi-sample transparency and strain-resistance measurements and observe a one-to-one correlation between them (Fig. 2(d)). Significantly larger error bars for the multi-sample characterization compared to straining are observed that emphasize the potential of our approach.

Our method does not rely on any assumptions about the sample morphology or dimensionality and can thus be employed for a wide variety of materials and conditions. We find that even compressive strain can be modelled with our approach (Fig. 3(a)). In the case of zero-dimensional nanoparticles in composites the model correctly predicts a decrease in resistance upon compressive strain which suggests that conduction indeed proceeds mainly through the fillers whose percolation pathway is effectively shortened. We also demonstrate that the model is not only applicable for different materials but also for a large range of applied strain and resistances. When characterizing a three-dimensional dispersion of two-dimensional graphene nanoplatelets in a polydimethylsiloxane (PDMS) matrix we observe good agreement over strain ranges of 40% and resistance variations of 7 orders of magnitude, as is shown in Fig. 3(b). The good agreement also demonstrates the limited impact of transverse strain and validates our initial assumption about the exclusive deformation of the dielectric matrix and the shape retention of the conductive constituents.

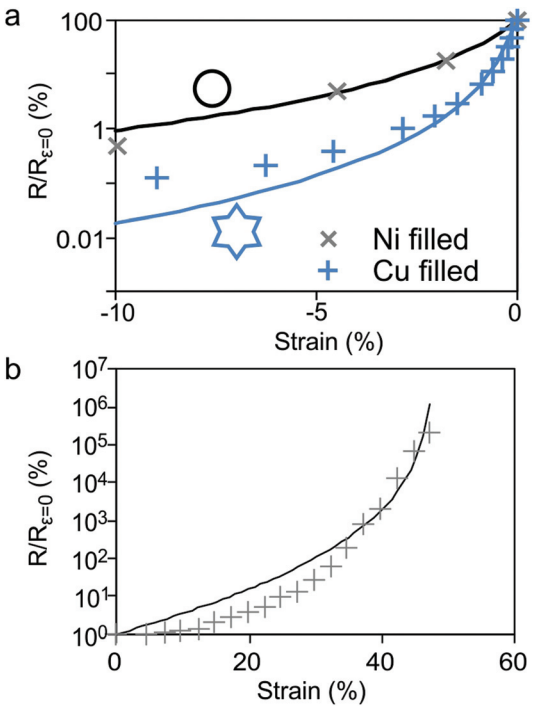

Fig. 3 Normalized strain–resistance diagrams and fits to eqn (4) for different material types: (a) strain response of two types of nanoparticle-filled polymers under compressive strain[31] and (b) graphene-derivative filled polymer[32] (more details about the samples are provided in the ESI†).

One of the important applications of our model is the extraction of the percolation exponent from strain–resistance curves. This exponent represents a measure of the connectivity between adjacent constituents and is expected to depend on the constituent shape and the sample morphology. A difference in the percolation exponent can thus be employed to identify the difference in the structure of the nanoscopic constituents. Fig. 3(a) shows the resistance–strain plots of two different particle types, Cu and Ni. According to our analysis, the percolation exponents differ significantly, with the Cu particles having a higher percolation exponent (about 2.7) compared to Ni particles (about 2.0). This difference is due to the peculiar shape of the Cu particles which show protruding sharp tips while the Ni particles being spherical.[30]

In addition to providing an enhanced characterization method we demonstrate that the strain-induced change in resistance is a suitable tool for comparing the assemblies of different nanomaterials. Traditionally, the comparison of different conductive films is accomplished by introducing a universal figure of merit. Coleman *et al.* suggested such a FOM,[8] termed Π, for percolative materials that relates two measurable quantities, resistance and transparency. Unfortunately, the figure of merit depends on the bulk equivalent thickness t_{min} according to

$$\Pi = 2\left[\frac{\sigma_{bulk}/\sigma_{Op}}{(Z_0 t_{min}\sigma_{Op})^n}\right]^{1/(n+1)} \quad (5)$$

This parameter cannot be directly extracted from the resistance or transparency measurements but again requires the comparison of multiple samples.

Our strain-based approach, on the other hand, allows us to calculate the FOM using the extracted values for R_0 and n, from an individual sample without the additional evaluation of t_{min} according to

$$\Pi = \left[\frac{L_0 Z_0}{(T^{-1/2}-1)^{n+1} W_0 R_0}\right]^{1/(n+1)} \quad (6)$$

This approach is validated by our observation of a good agreement of the thus extracted FOM values with multi-sample measurements (Fig. 4(a)) despite the large variations in the resistance of those samples. Moreover, considering that the FOM can span several orders of magnitude[8] the observed sample-to-sample variation is relatively small.

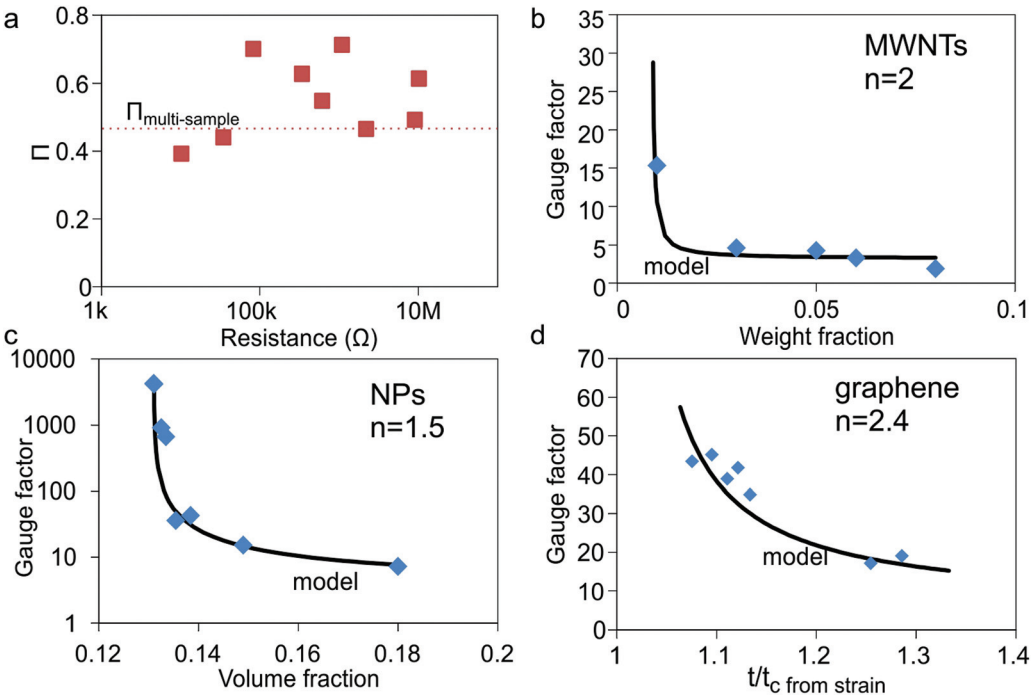

Fig. 4 (a) Figure of merit extracted from single-sample measurements of graphene films deposited at different substrate temperatures, (b–d) gauge factor evolution and fit to eqn (8) with sample concentration in terms of weight (b), conductive volume (c) and normalized film thickness (d) for different materials, *i.e.* (b) multi-walled nanotube filled polymer,[33] (c) nanoparticle-filled polymer,[13] and (d) flake graphene film[10,27] (more details about the samples are provided in the ESI†).

Finally, we apply the gained understanding to the research area of nanomaterial-based percolative strain gauges which exhibit a morphology-dependent sensitivity that is not observed in bulk strain gauges. Based on the definition of the gauge factor and eqn (4), we obtain:

$$\mathrm{GF} = \frac{R(\varepsilon) - R_0}{R_0}/\varepsilon = \left((1+\varepsilon)^2\left(\frac{t_0 - t_c}{t(\varepsilon) - t_c}\right)^n - 1\right)/\varepsilon \qquad (7)$$

Since the gauge factor is experimentally obtained for small strain values this formula can be simplified to

$$\mathrm{GF} \approx 2 + (1-\mu)n + (1-\mu)n\gamma \qquad (8)$$

where $\gamma = \frac{t_c}{t - t_c}$ and μ is the Poisson ratio of the material or substrate.

Using eqn (8), we fit several types of experimental data of strain gauge with small strain, *e.g.* multiwall carbon nanotube composites (Fig. 4(b)),[33] nanoparticles in a polymer matrix (Fig. 4(c)),[13] and graphene flake films (Fig. 4(d)).[10,27] We observe an excellent agreement of the simple formula with the experimental data despite its diverse nature. For example, the percolation exponent extracted from graphene flake films (n = 2.4) agrees well with the parameter extracted from the multi-sample FOM characterization.

When inspecting eqn (8), it is evident that the highest GF is achieved when the thickness is close to t_c under which conditions its magnitude is limited by γ and n. The parameter γ represents the relative difference in the thickness from the critical thickness and tends to infinity at t_c. In reality such high values for GF are not achievable, since straining of a film of critical thickness will break the last conductive pathway and transition to an insulator occurs. Instead, the highest value for GF is limited by the amount of strain that the sample needs to sustain but is as high as 168 for 1% strain. For identical preselected strain values, *i.e.* a fixed gamma, the difference in strain gauge sensitivity for different materials is completely determined by the variation of the percolation exponent. From predictions for n we identify that three-dimensional assemblies are expected to outperform two-dimensional films as strain gauges.

Conclusions

In conclusion, we have demonstrated a novel method to extract important percolation parameters by analyzing the strain-induced change in the resistance of percolative nanomaterials. A simple analytical formula shows good agreement with a wide variety of experimental data and allows characterization of the critical thickness and percolation exponent from single-sample measurements. The thus obtained parameters can be related to the previously used figures of merit for transparent conductors and strain gauges and show good agreement with traditional measurements. These results highlight the usefulness of our approach for the characterization of percolative nanomaterials for material optimization and future applications.

Conflicts of interest

There are no conflicts to declare.

Acknowledgements

M.H. acknowledges the funding from the Ministry of Science and Technology (MOST 107-2112-M-002-004-MY3). Y.H. acknowledges funding from MOST (107-2119-M-001-032-MY3) and Academia Sinica (SC1070201).

Notes and references

1 Z. N. Yu, L. Tetard, L. Zhai and J. Thomas, *Energy Environ. Sci.*, 2015, **8**, 702–730.
2 N. N. Jason, M. D. Ho and W. L. Cheng, *J. Mater. Chem. C*, 2017, **5**, 5845–5866.
3 N. Saito, H. Haniu, Y. Usui, K. Aoki, K. Hara, S. Takanashi, M. Shimizu, N. Narita, M. Okamoto, S. Kobayashi, H. Nomura, H. Kato, N. Nishimura, S. Taruta and M. Endo, *Chem. Rev.*, 2014, **114**, 6040–6079.
4 X. Cao, H. Chen, X. Gu, B. Liu, W. Wang, Y. Cao, F. Wu and C. Zhou, *ACS Nano*, 2014, **8**, 12769–12776.
5 R. M. Mutiso, M. C. Sherrott, A. R. Rathmell, B. J. Wiley and K. I. Winey, *ACS Nano*, 2013, **7**, 7654–7663.
6 A. Kumar and G. U. Kulkarni, *J. Appl. Phys.*, 2016, **119**, 015102.
7 W. Bauhofer and J. Z. Kovacs, *Compos. Sci. Technol.*, 2009, **69**, 1486–1498.
8 S. De, P. J. King, P. E. Lyons, U. Khan and J. N. Coleman, *ACS Nano*, 2010, **4**, 7064–7072.
9 P. N. Nirmalraj, P. E. Lyons, S. De, J. N. Coleman and J. J. Boland, *Nano Lett.*, 2009, **9**, 3890–3895.
10 Z. Chen, T. Ming, M. M. Goulamaly, H. M. Yao, D. Nezich, M. Hempel, M. Hofmann and J. Kong, *Adv. Funct. Mater.*, 2016, **26**, 5061–5067.
11 S. Sorel, P. E. Lyons, S. De, J. C. Dickerson and J. N. Coleman, *Nanotechnology*, 2012, **23**, 185201.
12 C. F. Ge and K. Cosgrove, *J. Electrost.*, 2015, **77**, 157–162.
13 T. D. Gupta, T. Gacoin and A. C. H. Rowe, *Adv. Funct. Mater.*, 2014, **24**, 4522–4527.
14 L. Chen, G. Chen and L. Lu, *Adv. Funct. Mater.*, 2007, **17**, 898–904.
15 S. De, P. J. King, M. Lotya, A. O'Neill, E. M. Doherty, Y. Hernandez, G. S. Duesberg and J. N. Coleman, *Small*, 2010, **6**, 458–464.
16 P. E. Lyons, S. De, J. Elias, M. Schamel, L. Philippe, A. T. Bellew, J. J. Boand and J. N. Coleman, *J. Phys. Chem. Lett.*, 2011, **2**, 3058–3062.
17 N. McEvoy, N. Peltekis, S. Kumar, E. Rezvani, H. Nolan, G. P. Keeley, W. J. Blau and G. S. Duesberg, *Carbon*, 2012, **50**, 1216–1226.
18 D. Stauffer and A. Aharony, *Introduction to percolation theory: revised second edition*, CRC press, 2014.
19 N. Johner, C. Grimaldi, I. Balberg and P. Ryser, *Phys. Rev. B: Condens. Matter Mater. Phys.*, 2008, **77**, 174204.
20 D. Toker, D. Azulay, N. Shimoni, I. Balberg and O. Millo, *Phys. Rev. B: Condens. Matter Mater. Phys.*, 2003, **68**, 204–213.
21 B. Nigro, C. Grimaldi and P. Ryser, *Phys. Rev. E: Stat., Nonlinear, Soft Matter Phys.*, 2012, **85**, 011137.
22 S. Vionnetmenot, C. Grimaldi, T. Maeder, S. Straessler and P. Ryser, *Phys. Rev. B: Condens. Matter Mater. Phys.*, 2005, **71**, 064201.
23 G. Ambrosetti, N. Johner, C. Grimaldi, T. Maeder, P. Ryser and A. Danani, *J. Appl. Phys.*, 2009, **106**, 953.
24 G. Li, S. D. Reis, A. A. Moreira, S. Havlin, H. E. Stanley and J. S. Andrade Jr., *Phys. Rev. E: Stat., Nonlinear, Soft Matter Phys.*, 2013, **87**, 042810.
25 A. A. Saberi, *Phys. Rep.*, 2015, **578**, 1–32.
26 O. Kanoun, C. Muller, A. Benchirouf, A. Sanli, T. N. Dinh, A. Al-Hamry, L. Bu, C. Gerlach and A. Bouhamed, *Sensors*, 2014, **14**, 10042–10071.
27 M. Hempel, D. Nezich, J. Kong and M. Hofmann, *Nano Lett.*, 2012, **12**, 5714–5718.
28 M. Hempel, D. Nezich, J. Kong and M. Hofmann, *Nano Lett.*, 2012, **12**, 5714–5718.
29 S. Mertens and C. Moore, *Phys. Rev. E: Stat., Nonlinear, Soft Matter Phys.*, 2012, **86**, 061109.
30 S. Stassi, G. Canavese, V. Cauda, S. L. Marasso and C. F. Pirri, *Nanoscale Res. Lett.*, 2012, **7**, 1–5.
31 S. Stassi, V. Cauda, G. Canavese and C. F. Pirri, *Sensors*, 2014, **14**, 5296–5332.
32 D. Ponnamma, Q. P. Guo, I. Krupa, M. A. S. Al-Maadeed, K. T. Varughese, S. Thomas and K. K. Sadasivuni, *Phys. Chem. Chem. Phys.*, 2015, **17**, 3954–3981.
33 G. T. Pham, Y. B. Park, Z. Liang, C. Zhang and B. Wang, *Composites, Part B*, 2008, **39**, 209–216.